Green Chemistry

PAPER

View Article Online
View Journal

Cite this: DOI: 10.1039/d6gc00954a

Optimized green extraction of multifunctional aliphatic and aromatic compounds from suberin-rich agro-industrial potato peel waste

Pedro Florido-Moreno, [a] Diego Rodríguez-Rodríguez,[a] José J. Benítez,[b] Jorge Rencoret, [c] Ekram Wassel,[d] Ruth E. Stark, [d] Susana Guzmán-Puyol, [a] José A. Heredia-Guerrero*[a] and José C. del Río [c]

Suberin-rich potato peel waste from the food industry was explored as a renewable source of multifunctional aliphatic and aromatic compounds. A green extraction methodology, consisting of an initial water-based extraction followed by alkaline hydrolysis with NaOH, was optimized by varying reaction time (2, 4, 6, and 8 h), temperature (40, 55, 70, 85, and 100 °C), and base concentration (0.1, 0.5, and 1 M). Response surface methodology revealed a strong combined effect of temperature and reaction time, identifying 0.5 M NaOH, 85 °C and 2 h as optimal conditions that balanced recovery yield and process sustainability. The composition of the hydrolysates was thoroughly characterized by gas chromatography-mass spectrometry (GC-MS). For comparison, a classic methanolysis protocol using extractive-free potato peels was also applied. In both approaches, the predominant compound families identified were α,ω-dicarboxylic acids and ω-hydroxy fatty acids, with octadec-9-ene-1,18-dioic acid and 18-hydroxyoctadec-9-enoic acid, respectively, as the most abundant components. Additional compound classes included fatty acids, fatty alcohols, monoglycerides, and aromatic derivatives. Unlike the classic method, which results in partial methylation of the carboxylic groups, the green method preserves these functionalities, therefore improving their suitability as potential building blocks for polymer synthesis, as demonstrated by melt-polycondensation for the fabrication of polymer coatings on aluminum substrates. The glycoalkaloids α-solanine and α-chaconine, naturally present in potato peels and highly toxic to humans, were largely removed during processing, as α-solanine was not detected and only trace amounts of α-chaconine could be found in both hydrolysates, likely due to their removal during the extraction steps and precipitation of the remainder under high-pH conditions.

Received 12th February 2026,
Accepted 7th April 2026

DOI: 10.1039/d6gc00954a

rsc.li/greenchem

Green foundation

1. This work contributes to green chemistry by developing and optimizing an aqueous NaOH-based method to extract multifunctional suberin-derived compounds from potato peel waste, offering a safer and more sustainable alternative to traditional organic solvent-based methanolysis.
2. The process avoids flammable solvents and hazardous reagents, significantly reduces glycoalkaloids to trace levels, and preserves carboxylic groups without methylation, enhancing their reactivity for polymer synthesis. Under optimized conditions (0.5 M NaOH, 85 °C, and 2 h), the method achieved up to 25% yield relative to dry biomass.
3. Further greening could involve replacing alkaline hydrolysis with enzymatic depolymerization using cutinases or esterases. These biocatalysts may allow depolymerization under milder, near-neutral conditions, increase selectivity for ester bonds, reduce energy consumption, and improve the environmental profile of the process within an integrated biorefinery framework.

[a]*Instituto de Hortofruticultura Subtropical y Mediterránea La Mayora, Consejo Superior de Investigaciones Científicas-Universidad de Málaga (IHSM, CSIC-UMA), Bulevar Louis Pasteur 49, Malaga, 29010, Spain. E-mail: ja.heredia@csic.es*
[b]*Instituto de Ciencia de Materiales de Sevilla, Centro Mixto CSIC-Universidad de Sevilla, Calle Americo Vespucio 49, Isla de la Cartuja, Sevilla, 41092, Spain*
[c]*Instituto de Recursos Naturales y Agrobiología de Sevilla, CSIC, Avda. Reina Mercedes, 10, Seville, 41012, Spain*
[d]*Department of Chemistry and Biochemistry, The City College of New York, City University of New York, and CUNY Institute for Macromolecular Assemblies, 85 Saint Nicholas Terrace, New York, New York 10031, USA*

Introduction

The quest for renewable sources of compounds with potential in various applications from otherwise discarded agricultural waste and food by-products is a key aspect of the circular bioeconomy.[1–3] Agro-industrial residues such as fruit peels, cereal husks, and vegetable pomaces are increasingly recognized as valuable feedstocks for the extraction of bioactive compounds, dietary fibers, pigments, and biopolymers.[4] This

valorization not only mitigates environmental impact associated with waste disposal but also contributes to the development of sustainable materials for food, pharmaceutical, and packaging industries. Among these residues, the discarded potato peel from the food industry stands out due to its high content of valuable molecules.[5,6] It is the primary solid by-product generated during industrial potato peeling, particularly during the production of chips, fries, and dehydrated flakes. It consists mainly of peels with a very small fraction of residual pulp. Around 0.16 tons of this material are produced per ton of processed potato.[7] Traditionally considered a low-value waste, potato peels are now seen as a valuable resource, with global production estimated at 70 000 to 140 000 tons per year. This waste is especially rich in phenolic compounds and specialized plant biopolymers such as suberin.[5,7]

Suberin is a complex hydrophobic biopolyester, composed of a poly(phenolic) and a poly(aliphatic) domain, which plays a crucial physiological role in plant defense and water balance.[8] It is predominantly deposited in the cell walls of specialized tissues such as the periderm, endodermis, and wound-healing layers, where it acts as a protective barrier. Suberin restricts the uncontrolled movement of water and solutes, prevents pathogen invasion, and minimizes mechanical damage. Its poly(aliphatic) domain is composed of long-chain fatty acids (mainly α,ω-dicarboxylic acids and ω-hydroxy fatty acids that can be functionalized in mid-positions with double bonds, diols, and epoxy groups), fatty alcohols, glycerol and derivatives, and phenolic compounds (in particular, ferulic acid) cross-linked into a polyester matrix, Fig. 1.[9] The monomeric constituents of the suberin poly(aliphatic) domain have attracted increasing interest for their potential in the development of sustainable materials.[9,10] Upon depolymerization, these suberin-derived monomers can serve as precursors for the synthesis of bio-based polyesters, hydrophobic coatings, adhesives, and resins. Their unique chemical structures, combining hydrophobic aliphatic chains and aromatic structures with reactive functional groups, enable the design of materials with tailored barrier, antimicrobial, and/or hydrophobic properties. Moreover, several suberin monomers, mainly aromatic molecules, exhibit antioxidant or antibacterial activity, expanding their potential uses in food packaging, biomedical formulations, and agricultural applications.

Several methodologies have been developed for the isolation and depolymerization of suberin from plant sources. The most established approach involves exhaustive solvent extraction to remove extractives, followed by alkaline methanolysis using sodium methoxide in methanol under reflux conditions.[12] On the other hand, aqueous alkaline hydrolysis is a methodology traditionally used for the chemical determination of suberin monomers[13] that offers a greener and safer alternative by avoiding flammable solvents, though it may lead to partial degradation of base-sensitive molecules. More

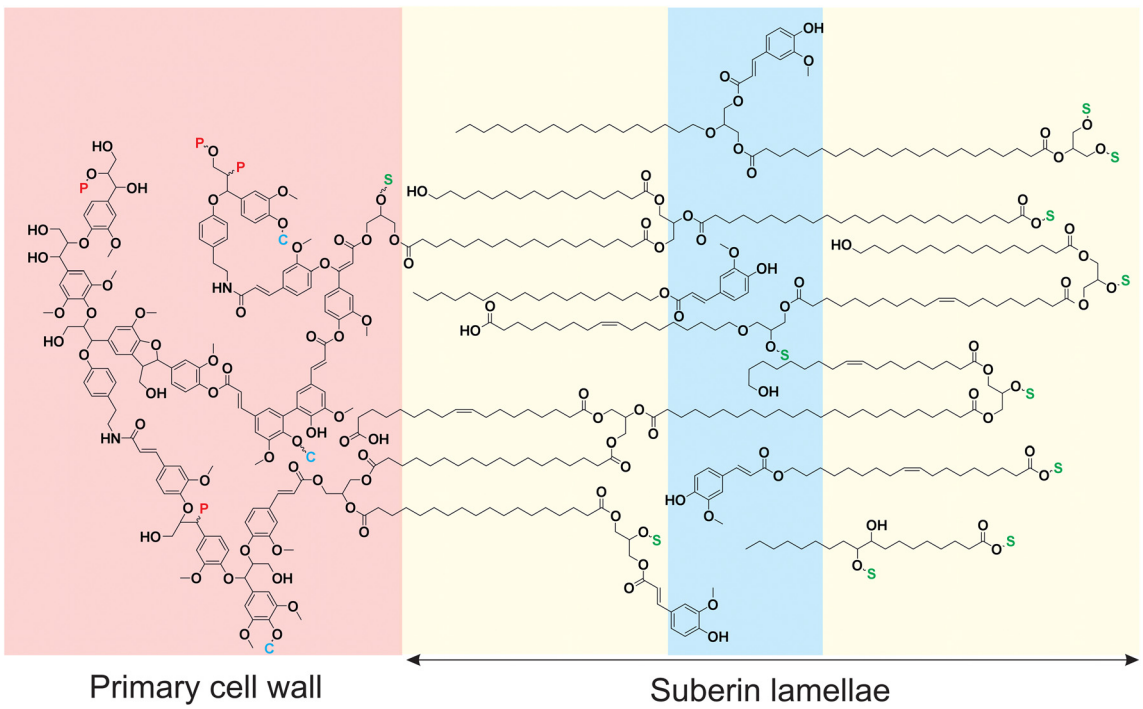

Fig. 1 Schematic representation of the proposed chemical architecture of potato suberin adapted from ref. 11, highlighting its biphasic nature with an aromatic (polyphenolic) domain associated with the primary cell wall and an aliphatic, glycerol-based polyester domain organized in lamellae. The structure of the poly(aliphatic) domain is mainly composed of long-chain fatty acids, ω-hydroxyacids, α,ω-dicarboxylic acids, glycerol, and phenolic moieties interconnected through ester linkages. These ester bonds constitute the primary cleavage sites during alkaline hydrolysis, enabling the release of multifunctional aliphatic and aromatic building blocks. The model illustrates a simplified two-dimensional section of the three-dimensional suberin network. C (in blue): carbohydrate; P (in red): phenolic; and S (in green): suberin (phenolic or aliphatic).

recently, ionic liquids have emerged as powerful media for suberin solubilization and mild depolymerization due to their ability to disrupt hydrogen bonding networks and ester linkages while preserving sensitive moieties.[14,15] Additionally, steam-explosion has also been explored to depolymerize suberin, offering a scalable and environmentally benign alternative, though partial hydrolysis and limited chemical integrity of labile functional groups remain challenges.[16] The choice of the depolymerization method significantly influences the yield, purity, and composition of the recovered suberin monomers, making method selection critical depending on the target application.

Potato peels are known to accumulate glycoalkaloids, predominantly α-solanine and α-chaconine, which serve as natural defense compounds against pests and pathogens.[5] These secondary metabolites are primarily localized in the outer layers of the tuber and their concentration can be influenced by factors such as the potato variety, cultivation conditions, and storage practices. Although essential for plant protection, elevated levels of glycoalkaloids pose concerns for human health due to their toxicity.[17] Therefore, proper handling and processing of potato peel by-products are critical to mitigate the risks associated with glycoalkaloid exposure and to enable their valorization in food or material applications. Several strategies have been explored to reduce the glycoalkaloid content in potato-derived materials, particularly in the peels. An effective removal strategy is achieved through solvent extraction, typically using chloroform/methanol or water/acetic acid mixtures, which can dissolve glycoalkaloids and facilitate their removal from the plant matrix.[18] Ultrasound-assisted extraction has been employed to reduce extraction times as well as energy and solvent consumption, while increasing glycoalkaloid recovery yields.[19] In addition, alkaline conditions have been reported to precipitate glycoalkaloid structures, representing a promising approach for detoxification of potato processing residues.[20,21]

In this work, we report a sustainable approach for the valorization of suberin-rich potato peels, a by-product from the food processing industry, through the development and optimization of a green extraction methodology for the recovery of multifunctional aliphatic and aromatic molecules. The process involves a preliminary aqueous extraction step followed by alkaline hydrolysis using sodium hydroxide, with systematic variation of reaction time, temperature, and base concentration to identify optimal conditions. The chemical composition of the resulting hydrolysates was analyzed comprehensively using gas chromatography-mass spectrometry (GC-MS) and compared with that obtained through a conventional methanolysis protocol applied to extractive-free potato peels. Particular attention was paid to evaluating the reduction of toxic glycoalkaloids under alkaline conditions.

Experimental part

Materials

Potato tubers (*Solanum tuberosum* L., cv. Agria), cultivated under field conditions in Seville, Spain, were kindly supplied by El Tío Las Papas S.L., a local potato chip manufacturer. During the industrial processing by this company, potato peels are generated as a by-product from the abrasive peeling of the tubers. Prior to use, peels were thoroughly washed with water to remove surface residues and subsequently air-dried.

Sodium metal, methanol, and dichloromethane were purchased from Sigma-Aldrich. Sodium hydroxide pellets and ethanol were obtained from Panreac. Ultrapure water (Milli-Q grade) was used in all procedures.

Preparation of suberin-rich hydrolysates

To hydrolyze and characterize the chemical composition of potato peels, two methodologies were employed. On one hand, a "classic", well-established protocol used for potato periderm was applied. This method involves exhaustive removal of extractives using various solvents, followed by $NaOCH_3$ methanolysis.[12] On the other hand, a novel, "green" approach is proposed in this study, based on the removal of water-soluble extractives and subsequent alkaline hydrolysis with NaOH. These are referred to throughout the manuscript as the classic and green methods, respectively.

Classic method. Potato peels were ground using a coffee grinder and sieved to obtain a particle size between 0.25 and 0.42 mm. The selected fraction was subjected to sequential extraction with a Soxhlet apparatus (ENDO Glassware, Spain) equipped with a 125 mL extractor, a Dimroth condenser, a 250 mL round-bottom flask, and a 36 × 22 × 80 mm extraction thimble with four solvents in the following order: dichloromethane (8 h), ethanol (18 h), water (24 h), and methanol (18 h), to ensure thorough removal of extractives of different polarity. The extractive-free peels were dried overnight at 40 °C. Subsequently, 500 mg of this material was hydrolyzed under reflux for 3 h in 50 mL of a 12 mM $NaOCH_3$ solution in methanol, prepared by dissolving metallic sodium directly in the solvent. The resulting mixture was filtered through a 0.45 μm syringe filter (PES membrane, 30 mm diameter, LLG Labware, Germany) and washed sequentially with 25 mL of methanol and 25 mL of chloroform. The final solid was dried under a fume hood for 24 h. As discussed below, sodium methoxide induces partial methylation of carboxylic acid groups, converting them into methyl esters, which enhances compound volatility and chromatographic behavior, thereby facilitating their detection and identification by GC-MS.

Green method. Potato peels were similarly ground and sieved to obtain a particle size of 0.25–0.42 mm. The selected fraction was extracted in a Soxhlet apparatus (ENDO Glassware, Spain) with water for 24 h to remove water-soluble components and then dried overnight at 40 °C. The objective of this water extraction step is to remove low-molecular-weight sugars, organic acids, amino acids, and inorganic salts. This pretreatment was performed to minimize analytical interference and to improve the selectivity of the subsequent depolymerization process. Although these hydrophilic components are not covalently bound to the suberin matrix and therefore do not directly affect suberin cleavage, their presence may complicate chromatographic analysis, introduce extraneous

peaks in GC-MS profiles, and promote undesired side reactions under alkaline conditions. The removal of water-soluble extractives thus ensures a more accurate characterization of suberin-derived monomers while preserving the structural integrity of the polymeric suberin domain. In addition, the presence of these water-soluble extractives could interfere with subsequent melt polycondensation, as they may act as chain terminators, inhibit esterification reactions, and promote undesired side processes, ultimately affecting polymer growth and coating homogeneity. Alkaline hydrolysis was performed under reflux using 500 mg of the water-extracted peels in 50 mL of NaOH solution. Reaction conditions were optimized by varying time (2, 4, 6, and 8 h), temperature (40, 55, 70, 85, and 100 °C), and NaOH concentration (0.1, 0.5, and 1 M). After hydrolysis, the mixtures were neutralized with concentrated HCl (37%), leading to the precipitation of a brownish solid. The precipitates were washed twice with 25 mL of water to remove residual NaCl and dried under a fume hood for 24 h.

In both methods, the recovery yield was determined. It represents the percentage of material solubilized and recovered after hydrolysis relative to the initial dry weight of extractive-free potato peels (only the water-soluble extractives in the case of the green method) used in the reaction. It provides an estimation of the efficiency of the hydrolytic process in releasing soluble compounds from the solid matrix. The recovery yield (%) was calculated using the following eqn (1):

$$\text{Yield}\,(\%) = \left(\frac{m_{\text{recovered}}}{m_{\text{initial}}}\right) \times 100 \qquad (1)$$

where $m_{\text{recovered}}$ is the mass of the dried hydrolysate (mg) obtained after filtration, washing, and drying and m_{initial} is the mass of the initial dry, extractive-free potato peels (only the water-soluble extractives in the case of the green method) subjected to hydrolysis (mg).

The hydrolysis conditions of the green method were optimized through a face centered composite design. Two independent variables, temperature (X_1, °C) and time (X_2, min), were selected for the experimental design, while the yield (%) was considered as the response. Four and five variation levels were chosen for time and temperature, respectively. Factors were coded as −1, −0.3333, +0.3333, and +1 for time and as −1, −0.5, 0, +0.5, and +1 for temperature, Table S1. The statistical experimental design and optimization calculations were performed using R software (v3.63, https://www.r-project.org). The responses and variables were correlated by response surface analysis to obtain the coefficients of the following quadratic equation:

$$Y = \beta_0 + \sum_{i=1}^{k} \beta_i x_i + \sum_{i=1,i<j}^{k=1} \sum_{j=2}^{k} \beta_{ij} x_j + \sum_{i=2}^{k} \beta_{ii} {x_{ii}}^2 \qquad (2)$$

where β_0, β_i, β_{ii}, and β_{ij} are the regression coefficients, x_i and x_j are the coded levels of independent variables affecting the dependent response Y and k is the number of parameters.

Analysis of the monomeric compounds by gas chromatography-mass spectrometry (GC-MS)

The hydrolysates were analyzed by GC-MS after derivatization with *N*,*O*-bis(trimethylsilyl)trifluoroacetamide (BSTFA) to form their trimethylsilyl (TMS) ether derivatives. The analyses were performed on a Shimadzu QP 2010 Ultra GC-MS system (Kyoto, Japan) using a fused-silica DB-5HT capillary column (30 m length × 0.25 mm i.d., 0.1 μm film thickness) from J&W Scientific (Folsom, CA, USA). The oven was heated from 120 °C (1 min) to 300 °C at 5 °C min^{-1} and held for 15 min. The injection was performed at 300 °C and the transfer line was kept at 300 °C. Helium was used as the carrier gas at a rate of 1 mL min^{-1}. The different compounds were identified by comparison of their mass spectra with those in the NIST library, by comparison with the literature[12,22] and, when possible, by comparison with authentic standards.

Analysis of α-solanine and α-chaconine by solution-state nuclear magnetic resonance spectroscopy (NMR)

The presence of the glycoalkaloids α-solanine and α-chaconine in the hydrolysates was established using 2D-NMR spectroscopy. The analyses were performed on a Bruker Avance III 500 MHz spectrometer (Bruker, Karlsruhe, Germany) equipped with a 5 mm TCI cryoprobe. Pure standards of α-solanine and α-chaconine were also served as references. Approximately 40 mg of hydrolysate or 4 mg of the standard compound were dissolved in 0.6 mL of DMSO-d_6. Heteronuclear Single Quantum Coherence (HSQC) spectra were acquired using the standard "hsqcetpgsisp.2.2" pulse program. For the semiquantitative estimation, HSQC signal integration was performed using Bruker Topspin 4.2 software focusing on the distinctive anomeric carbon signals of the glycoalkaloids.

Polymerization of the suberin-rich hydrolysates

Ten milligrams of the suberin-rich hydrolysate obtained under optimized green hydrolysis conditions (0.5 M NaOH, 85 °C, 2 h) were dispersed in 10 mL of a water/ethanol mixture (9 : 1 v/v) under magnetic stirring at 1600 rpm for 10 min. Subsequently, 0.15 mL of the dispersion was electrosprayed onto an aluminum substrate (4 × 4 cm^2) using a Spinbox electrospray system (Fluidnatek, Spain) operated at a voltage of 17 kV, a tip-to-substrate distance of 5 cm, and a flow rate of 0.02 mL min^{-1}. The deposition step was repeated three times to ensure homogeneous film coverage. The resulting coatings were then subjected to thermal polymerization in an air-circulating oven at 175 °C for 60 min. For comparison, non-polymerized coatings were prepared following the same procedure but omitting the thermal curing step.

Colorimetric analysis

Color measurements of the coatings were performed in the CIELAB color space using a portable colorimeter (CR-10 Plus, Konica Minolta, Ramsey, USA), where L^* represents lightness (0 = black, 100 = white), a^* the green–red axis, and b^* the blue–yellow axis. A white calibration standard (L^* = 97.94, a^* = 0.22, b^* = 1.33) was used prior to measurements.

The total color difference (ΔE) between samples was calculated according to eqn (3):

$$\Delta E = \sqrt{(L^* - L_0^*)^2 + (a^* - a_0^*)^2 + (b^* - b_0^*)^2} \quad (3)$$

where L_0^*, a_0^*, and b_0^* correspond to the reference values of the unpolymerized coating.

The Browning Index (BI) was calculated using eqn (4) and (5):

$$\text{BI } (\%) = 100 \times (x - 0.31)/0.172 \quad (4)$$

where:

$$x = (a + 1.75\ \text{L})/(5.64\ \text{L} + a - 3.012b). \quad (5)$$

Attenuated total reflection-Fourier transform infrared (ATR-FTIR)

Infrared spectra were recorded using a Fourier-transform infrared spectrometer (model 6X, Jasco, Japan) equipped with a single-reflection attenuated total reflection (ATR) accessory (ProOne X, Jasco, Japan). Spectra were acquired in the range of 4000–600 cm^{-1} with a spectral resolution of 4 cm^{-1} and by averaging 128 scans per measurement. For each sample, spectra were collected from three different surface regions to ensure representativeness and reproducibility.

Solid state-nuclear magnetic resonance (ss-NMR)

The ^{13}C NMR measurements were performed on 3-5 mg of powdered samples at the New York Structural Biology Center, using as Brujer AVANCE NEO NMR spectrometer operating at a ^{13}C frequency of 225 MHz and equipped with a Varian (Agilent) 1.6 mm FastMAS probe spinning at 19.0 kHz. The chemical functionalities present in the polymerized coating were identified and estimated quantitatively by employing Direct Polarization Magic-Angle Spinning (DPMAS) experiments using a recycle delay of 50 s between 1250–1600 successive acquisitions, and a radiofrequency field strength of 90 kHz for ^1H decoupling. The ^{13}C and ^1H 90° pulse lengths were 2.5 and 2.8 μs, respectively. Spectral processing was carried out by applying line broadening of 150 Hz. Relative proportions of the main carbon types defined in the chemical shift region corresponding to carboxyl and ester groups (160–180 ppm) were estimated by deconvolution. Peak areas were determined using OriginLab image analysis software.

Results and discussion

Optimization of aqueous NaOH hydrolysis for suberin monomer recovery

To rigorously assess the effect of operating variables and their interactions, we applied a response surface methodology (RSM) for temperature (40–100 °C) and time (2–8 h) as independent factors. Separate quadratic models were fitted for each NaOH concentration (0.1, 0.5, and 1 M). The fitted surfaces are shown in Fig. 2, while the model coefficients can be found in Table S2. The resulting surfaces and contour plots revealed distinct behaviors depending on the alkali concentration. For the lowest concentration (0.1 M NaOH, Fig. 2A), the recovery yields remained below 7%, even under the most severe conditions. The model predicted a maximum of 6.8% at 100 °C and 2 h, confirming that the base acted as a limiting reagent, insufficient to promote extensive cleavage of the suberin polyester network. At 0.5 M NaOH (Fig. 2B), the response surface exhibited a pronounced curvature, indicating a strong combined effect of temperature and reaction time. The highest predicted yield (24.1%) was obtained at 62 °C and 8 h. However, comparable yields (>19%) were achieved even at shorter reaction times and higher temperatures, such as 85 °C and 2 h, which are more favorable in terms of energy and processing efficiency. In contrast, at 1 M NaOH (Fig. 2C), the surface became broader and less steep, suggesting that the reaction approached completion across a wider operational window. The predicted optimum point (22.8%) occurred at 80 °C and 2 h, indicating efficient hydrolysis even under relatively mild conditions. The marginal improvement in yield compared with that with 0.5 M NaOH (<3% points for 2 h of hydrolysis) did not compensate for the increased reagent consumption and potential environmental impact. Taken together, these models demonstrate that the hydrolysis efficiency increased with NaOH concentration but reached a plateau between 0.5 and 1 M. Considering both the predicted yields and process sustainability, 0.5 M NaOH, 85 °C, and 2 h were selected as the operating conditions for subsequent experiments, providing high recovery with reduced chemical input and shorter reaction time. In any case, the remaining mass fraction is largely associated with polysaccharide- and lignin-rich residues from the potato peel matrix.

Comparison of the chemical compositions of suberin hydrolysates extracted by the optimized green aqueous NaOH hydrolysis and the classic sodium methanolysis method

The hydrolysates resulting from the depolymerization of potato suberin using both the classic and the optimized green hydrolysis methods were dissolved in chloroform and subjected to GC-MS analysis. Fig. 3 shows the chromatograms of the hydrolysates obtained from both methods (classic and green) as their TMS-ether derivatives. The identities and abundances (as mg g^{-1} of hydrolysate) of the compounds identified are listed in Table 1. Representative structures of the different classes of compounds identified are shown in Fig. 4.

Different families of compounds were identified in the hydrolysates obtained by the classic and green methods, and their relative abundances, calculated from the data reported in Table 1, are presented in the histogram shown in Fig. 5. The most abundant in both hydrolysates was α,ω-dicarboxylic acids, reaching 427.64 mg g^{-1} of hydrolysate in the classic method and 398.99 mg g^{-1} in the green one. These were followed by ω-hydroxyfatty acids, with concentrations of 318.23 and 257.78 mg g^{-1} for the classic and green methods, respectively. Other families included fatty acids (104.50 and 170.43 mg g^{-1}), fatty alcohols (78.41 and 148.51 mg g^{-1}),

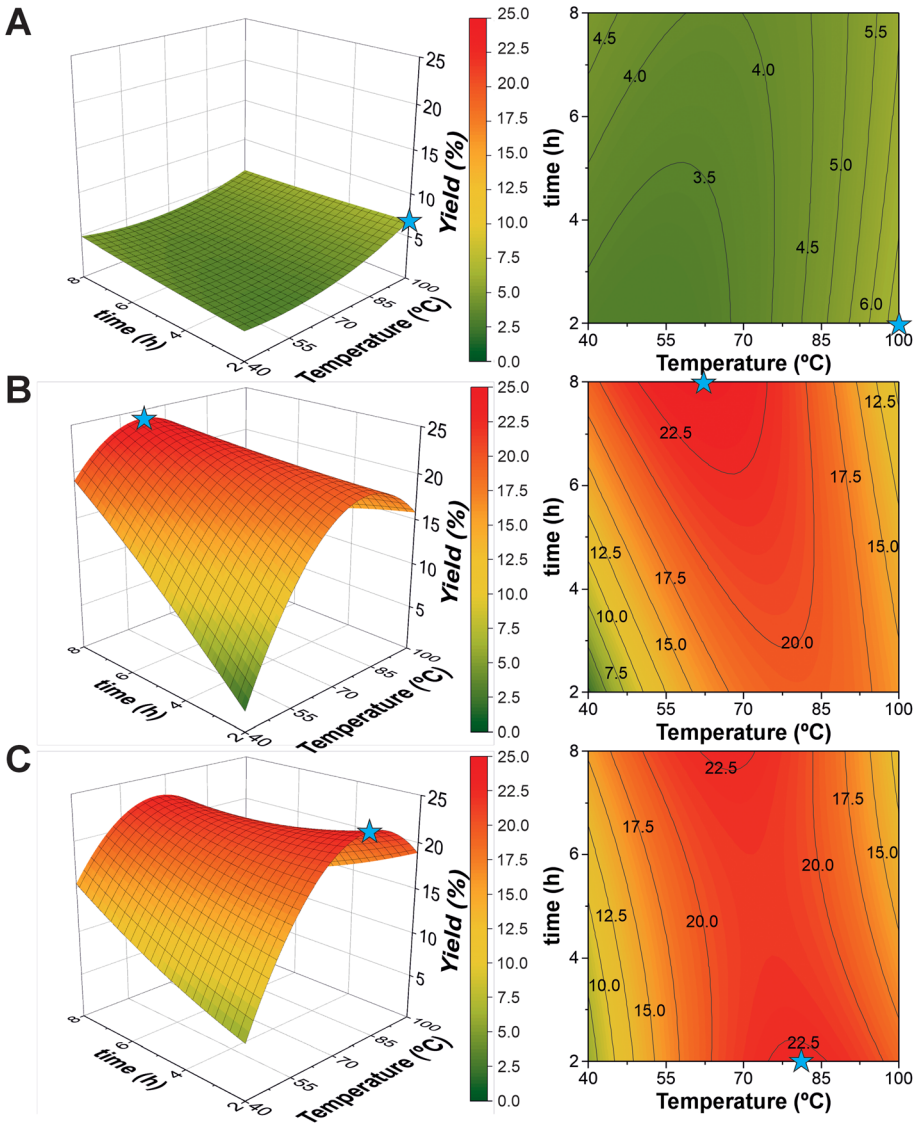

Fig. 2 Left, response surface plots and, right, contour graphs for the recovery yields of the alkaline hydrolysis of suberin-rich potato peel waste with time and temperature at different NaOH concentrations: (A) 0.1 M, (B) 0.5 M, and, (C) 1 M. The color scale refers to the yield percentage. Predicted optimum points have been highlighted with a blue star.

monoglycerides (42.07 and 3.52 mg g^{-1}), and aromatic compounds, including alkyl ferulates (29.14 and 20.78 mg g^{-1}), for the classic and green methods, respectively.

Notably, the green aqueous NaOH hydrolysis yielded higher amounts of free fatty acids and fatty alcohols compared to the classical methanolysis. This behavior can be attributed to the absence of organic solvent-based extraction during the pretreatment step, which in the classical protocol removes a significant portion of the lipophilic compounds, which are known to be present in potato peels,[23] prior to depolymerization. By omitting this extraction stage, the green method retains these components within the matrix, allowing their subsequent release during alkaline hydrolysis. Conversely, monoglycerides were reduced by more than 90% under green conditions, likely due to more extensive ester bond cleavage promoted by the aqueous alkaline medium. Such hydrolysis also contributes to the observed increase in free fatty acid content, as monoglycerides are converted into their corresponding fatty acids and glycerol units.

Importantly, the classic method (based on methanolysis with sodium methoxide that acts simultaneously as a strong nucleophile and transesterification catalyst) induces partial methylation of carboxylic acid groups, leading to the formation of methyl esters. This transesterification complicates the GC-MS interpretation, particularly for α,ω-dicarboxylic acids, which may appear as free acids, mono- or dimethyl esters, thereby increasing chromatographic complexity in interpretation and quantification. In contrast, the green NaOH hydrolysis preserves the free carboxylic functionalities of the released monomers, facilitating their identification and

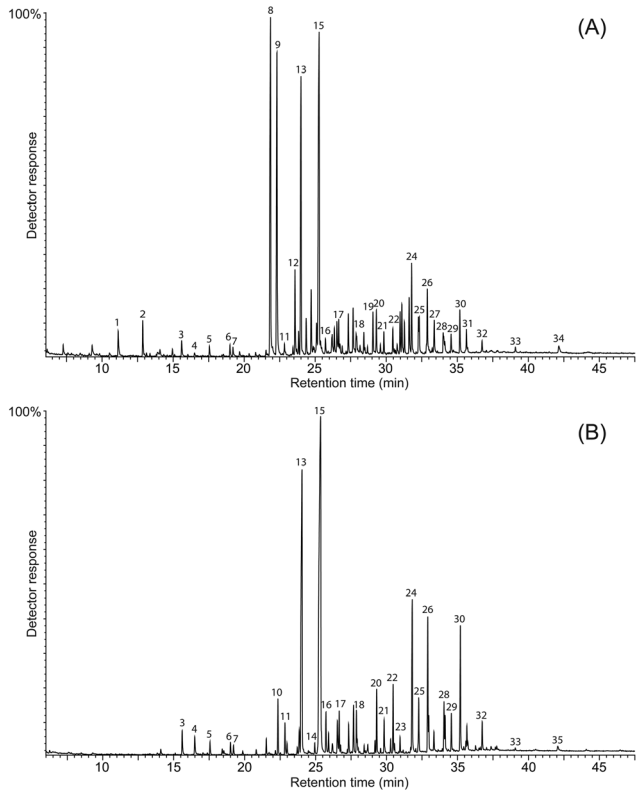

Fig. 3 GC-MS chromatograms of the TMS-ether derivatives of the compounds released after hydrolysis of potato suberin using (A) the classic methanolysis method and (B) the optimized, green hydrolysis one. Labels for selected compounds are **1**: nonane-1,9-dioic acid; **2**: quinic acid; **3**: *n*-hexadecanoic acid; **4**: ferulic acid; **5**: *n*-octadecanol; **6**: *n*-octadecanoic acid; **7**: *n*-nonadecanol; **8**: octadec-9-ene-1,18-dioic acid dimethyl ester; **9**: 18-hydroxyoctadec-9-enoic acid methyl ester; **10**: *n*-heneicosanol; **11**: hexadecane-1,16-dioic acid; **12**: octadec-9-ene-1,18-dioic acid monomethyl ester; **13**: 18-hydroxyoctadec-9-enoic acid; **14**: octadeca-9,12-dien-1,18-dioic acid; **15**: octadec-9-ene-1,18-dioic acid; **16**: octadecane-1,18-dioic acid; **17**: *n*-tetracosanol; **18**: *n*-tetracosanoic acid; **19**: *n*-hexacosanoic acid methyl ester; **20**: *n*-hexacosanol; **21**: 22-hydroxydocosanoic acid; **22**: *n*-hexacosanoic acid; **23**: docosane-1,22-dioic acid; **24**: *n*-octacosanol; **25**: 24-hydroxytetracosanoic acid; **26**: *n*-octacosanoic acid; **27**: 26-hydroxyhexacosanoic acid methyl ester; **28**: *n*-nonacosanoic acid; **29**: 26-hydroxyhexacosanoic acid; **30**: *n*-triacontanoic acid; **31**: 28-hydroxyoctacosanoic acid methyl ester; **32**: 28-hydroxyoctacosanoic acid; **33**: 30-hydroxytriacontanoic acid; **34**: 18-*O*-feruloyloxyoctadec-9-enoic acid methyl ester; and **35**: *n*-heneicosanyl ferulate.

enabling a more straightforward structural characterization. From a functional standpoint, the presence of unsubstituted carboxylic and hydroxyl groups substantially enhances the reactivity of the monomers in condensation reactions, making them more effective and versatile precursors for the synthesis of bio-based polyesters. This difference underscores not only the chemical selectivity and structural integrity achieved by the green method, but also its superior suitability for downstream polymerization and sustainable material design.

The most important monomeric compounds released using the classic method (Fig. 3A and Table 1) were octadec-9-ene-

Table 1 Composition and abundance (mg g^{-1} hydrolysate) of the compounds identified in the hydrolysates of potato suberin using the classic and the green methods. Roman numbers in parentheses refer to the structures depicted in Fig. 4

Compounds	Classic	Green
α,ω-Dicarboxylic acids	**427.64**	**398.99**
Octane-1,8-dioic acid	5.17	0.00
Nonane-1,9-dioic acid	8.90	0.32
Hexadecane-1,16-dioic acid	3.55	10.18
Hexadecane-1,16-dioic acid monomethyl ester	0.33	—
Hexadecane-1,16-dioic acid dimethyl ester	1.54	—
Octadeca-9,12-dien-1,18-dioic acid	1.44	3.39
Octadeca-9,12-dien-1,18-dioic acid monomethyl ester	0.00	—
Octadeca-9,12-dien-1,18-dioic acid dimethyl ester	0.48	—
Octadec-9-ene-1,18-dioic acid (**I**)	156.29	318.25
Octadec-9-ene-1,18-dioic acid monomethyl ester	23.31	—
Octadec-9-ene-1,18-dioic acid dimethyl ester	138.81	—
Hydroxyoctadec-9-ene-1,18-dioic acid (various isomers)	23.43	25.95
Hydroxyoctadec-9-ene-1,18-dioic acid monomethyl ester (various isomers)	2.74	—
Hydroxyoctadec-9-ene-1,18-dioic acid dimethyl ester (various isomers)	25.09	—
Octadecane-1,18-dioic acid	5.97	15.93
Octadecane-1,18-dioic acid monomethyl ester	0.33	—
Octadecane-1,18-dioic acid dimethyl ester	3.11	—
9,10-Dihydroxyoctadecane-1,18-dioic acid	2.64	1.63
9,10-Dihydroxyoctadecane-1,18-dioic acid monomethyl ester	0.80	—
9,10-Dihydroxyoctadecane-1,18-dioic acid dimethyl ester	1.87	—
Eicos-9-ene-1,20-dioic acid	1.20	0.72
Eicos-9-ene-1,20-dioic acid monomethyl ester	0.25	—
Eicos-9-ene-1,20-dioic acid dimethyl ester	0.57	—
Eicosane-1,20-dioic acid	1.03	3.39
Eicosane-1,20-dioic acid monomethyl ester	0.28	—
Eicosane-1,20-dioic acid dimethyl ester	1.18	—
Docosane-1,22-dioic acid	2.41	6.02
Docosane-1,22-dioic acid monomethyl ester	0.50	—
Docosane-1,22-dioic acid dimethyl ester	2.59	—
Tetracosane-1,24-dioic acid	3.01	7.99
Tetracosane-1,24-dioic acid monomethyl ester	0.51	—
Tetracosane-1,24-dioic acid dimethyl ester	3.45	—
Hexacosane-1,26-dioic acid	1.09	3.73
Hexacosane-1,26-dioic acid monomethyl ester	0.44	—
Hexacosane-1,26-dioic acid dimethyl ester	1.71	—
Octacosane-1,28-dioic acid	0.15	1.50
Octacosane-1,28-dioic acid monomethyl ester	0.23	—
Octacosane-1,28-dioic acid dimethyl ester	1.23	—
ω-Hydroxyfatty acids	**318.23**	**257.78**
16-Hydroxyhexadecanoic acid	1.73	3.80
16-Hydroxyhexadecanoic acid methyl ester	1.29	—
18-Hydroxyoctadeca-9,12-dienoic acid	1.22	2.18
18-Hydroxyoctadeca-9,12-dienoic acid methyl ester	1.42	—
18-Hydroxyoctadec-9-enoic acid (**II**)	97.61	164.71
18-Hydroxyoctadec-9-enoic acid methyl ester	116.34	—
Dihydroxyoctadec-9-enoic acid (various isomers)	15.18	17.12
Dihydroxyoctadec-9-enoic acid methyl ester (various isomers)	17.82	—
9,10,18-Trihydroxyoctadecanoic acid (**III**)	1.34	0.58
9,10,18-Trihydroxyoctadecanoic acid methyl ester	0.48	—
18-Hydroxyoctadecanoic acid	0.31	0.83
18-Hydroxyoctadecanoic acid methyl ester	0.46	—
20-Hydroxyeicosanoic acid	0.64	1.28
20-Hydroxyeicosanoic acid methyl ester	0.94	—
22-Hydroxydocosanoic acid	5.65	11.36
22-Hydroxydocosanoic acid methyl ester	5.60	—
24-Hydroxytetracosanoic acid	9.78	26.39
24-Hydroxytetracosanoic acid methyl ester	12.14	—

Table 1 *(Contd.)*

Compounds	Classic	Green
26-Hydroxyhexacosanoic acid	5.56	15.80
26-Hydroxyhexacosanoic acid methyl ester	10.54	—
28-Hydroxyoctacosanoic acid	3.35	12.40
28-Hydroxyoctacosanoic acid methyl ester	7.72	—
30-Hydroxytriacontanoic acid	0.56	1.34
30-Hydroxytriacontanoic acid methyl ester	0.57	—
Fatty acids	**104.50**	**170.43**
n-Tetradecanoic acid	0.20	0.49
n-Hexadecanoic acid	5.95	8.92
n-Heptadecanoic acid	0.10	0.26
Octadeca-9,12-dienoic acid	0.52	2.11
Octadec-9-enoic acid	0.81	1.96
n-Octadecanoic acid	3.62	4.37
n-Eicosanoic acid	0.33	1.64
n-Eicosanoic acid methyl ester	0.41	—
n-Heneicosanoic acid	0.23	0.54
n-Docosanoic acid	1.77	2.51
n-Docosanoic acid methyl ester	2.87	—
n-Tricosanoic acid	0.37	1.40
n-Tetracosanoic acid	4.70	15.42
n-Tetracosanoic acid methyl ester	6.01	—
n-Pentacosanoic acid	0.17	1.11
n-Hexacosanoic acid	7.26	20.38
n-Hexacosanoic acid methyl ester	11.82	—
n-Heptacosanoic acid	0.28	1.59
n-Octacosanoic acid (**IV**)	17.81	47.56
n-Octacosanoic acid methyl ester	16.75	—
n-Nonacosanoic acid	3.06	15.46
n-Triacontanoic acid	12.31	42.42
n-Triacontanoic acid methyl ester	6.07	—
n-Hentriacontanoic acid	0.13	1.50
n-Dotriacontanoic acid	0.70	0.77
n-Dotriacontanoic acid methyl ester	0.22	—
Fatty alcohols	**78.41**	**148.51**
n-Hexadecanol	2.09	2.29
n-Heptadecanol	0.14	0.13
n-Octadecanol	3.48	4.18
n-Nonadecanol	2.33	2.97
n-Eicosanol	1.04	1.59
n-Heneicosanol	15.08	15.84
n-Docosanol	6.20	9.30
n-Tricosanol	2.81	1.66
n-Tetracosanol	7.03	10.89
n-Pentacosanol	0.46	1.22
n-Hexacosanol	10.92	18.30
n-Heptacosanol	0.68	2.20
n-Octacosanol (**V**)	24.23	61.29
n-Nonacosanol	1.10	7.74
n-Triacontanol	0.84	8.92
Monoglycerides	**42.07**	**3.52**
Monoacylglyceryl esters of fatty acids		
1-Monohexadecanoylglycerol	0.50	0.74
1-Monooctadecanoylglycerol	1.00	2.78
1-Monoeicosanoylglycerol	0.11	0.00
1-Monodocosanoylglycerol	0.23	0.00
1-Monotetracosanoylglycerol	0.42	0.00
1-Monohexacosanoylglycerol	1.12	0.00
1-Monooctacosanoylglycerol (**VI**)	2.01	0.00
1-Monotriacontanoylglycerol	1.00	0.00
Monoacylglyceryl esters of α,ω-dicarboxylic acids		
2-Mono(octadec-9-ene-18-oic acid-oyl)glycerol	1.45	0.00
2-Mono(octadec-9-ene-18-oic acid-oyl)glycerol methyl ester	0.91	—
1-Mono(octadec-9-ene-18-oic acid-oyl)glycerol (**VII**)	10.40	0.00
1-Mono(octadec-9-ene-18-oic acid-oyl)glycerol methyl ester	14.15	—

Table 1 *(Contd.)*

Compounds	Classic	Green
Monoacylglyceryl esters of ω-hydroxyfatty acids		
2-Mono(18-hydroxyoctadec-9-enoyl)glycerol	0.78	0.00
1-Mono(18-hydroxyoctadec-9-enoyl)glycerol (**VIII**)	8.00	0.00
Aromatics	**29.14**	**20.78**
Vanillin	0.35	0.69
Vanillic acid (**IX**)	1.75	1.02
Vanillic acid methyl ester	2.25	—
Coniferyl alcohol	0.46	1.16
Ferulic acid (**X**)	2.25	8.02
Ferulic acid methyl ester	3.16	—
Caffeic acid (**XI**)	0.08	0.67
Quinic acid (**XII**)	10.84	0.28
Feruloyl esters		
Glycerol ferulate (**XIII**)	2.88	0.00
n-Hexadecyl ferulate	0.00	1.12
n-Octadecyl ferulate	0.00	1.04
n-Nonadecyl ferulate	0.00	0.42
n-Eicosanyl ferulate	0.00	0.34
n-Heneicosanyl ferulate	0.00	3.53
n-Docosanyl ferulate	0.00	0.87
n-Tricosanyl ferulate	0.00	0.73
n-Tetracosanyl ferulate	0.00	0.89
Feruloyl esters of ω-hydroxyfatty alcohols		
18-*O*-Feruloyloxyoctadec-9-enoic acid methyl ester (**XIV**)	5.12	—

1,18-dioic acid (peak 15, structure **I**) and 18-hydroxyoctadec-9-enoic acid (peak 13, structure **II**), alongside their methyl ester derivatives octadec-9-ene-1,18-dioic acid dimethyl ester (peak 8) and 18-hydroxyoctadec-9-enoic acid methyl ester (peak 9). Similarly, the most prominent monomeric compounds released using the green hydrolysis method (Fig. 3B and Table 1) were 18-hydroxyoctadec-9-enoic acid (peak 13) and octadec-9-ene-1,18-dioic acid (peak 15). These results are in agreement with those from previous studies.[12,22,24]

The series of α,ω-dicarboxylic acids was the most abundant class of compounds released by both methods. This series ranged from octane-1,8-dioic acid (C_8) to octacosane-1,28-dioic acid (C_{28}) with the exclusive occurrence of the even carbon atom numbered homologues, and also including unsaturated compounds such as octadec-9-ene-1,18-dioic acid (**I**), which was the most abundant compound in the series, as well as octadeca-9,12-dien-1,18-dioic acid and eicos-9-ene-1,20-dioic acid. Mid-chain monohydroxy and dihydroxy α,ω-dicarboxylic acids were also released, including 9,10-dihydroxyoctadecane-1,18-dioic acid and various isomers of hydroxyoctadec-9-ene-1,18-dioic acid.

The series of ω-hydroxyfatty acids were the second most abundant class of compounds released using both methods. This series ranged from 16-hydroxyhexadecanoic acid (C_{16}) to 30-hydroxytriacontanoic acid (C_{30}), with the exclusive occurrence of the even carbon atom numbered homologues, and including unsaturated compounds, such as 18-hydroxyoctadec-9-enoic acid (**II**), which was the most abundant one.

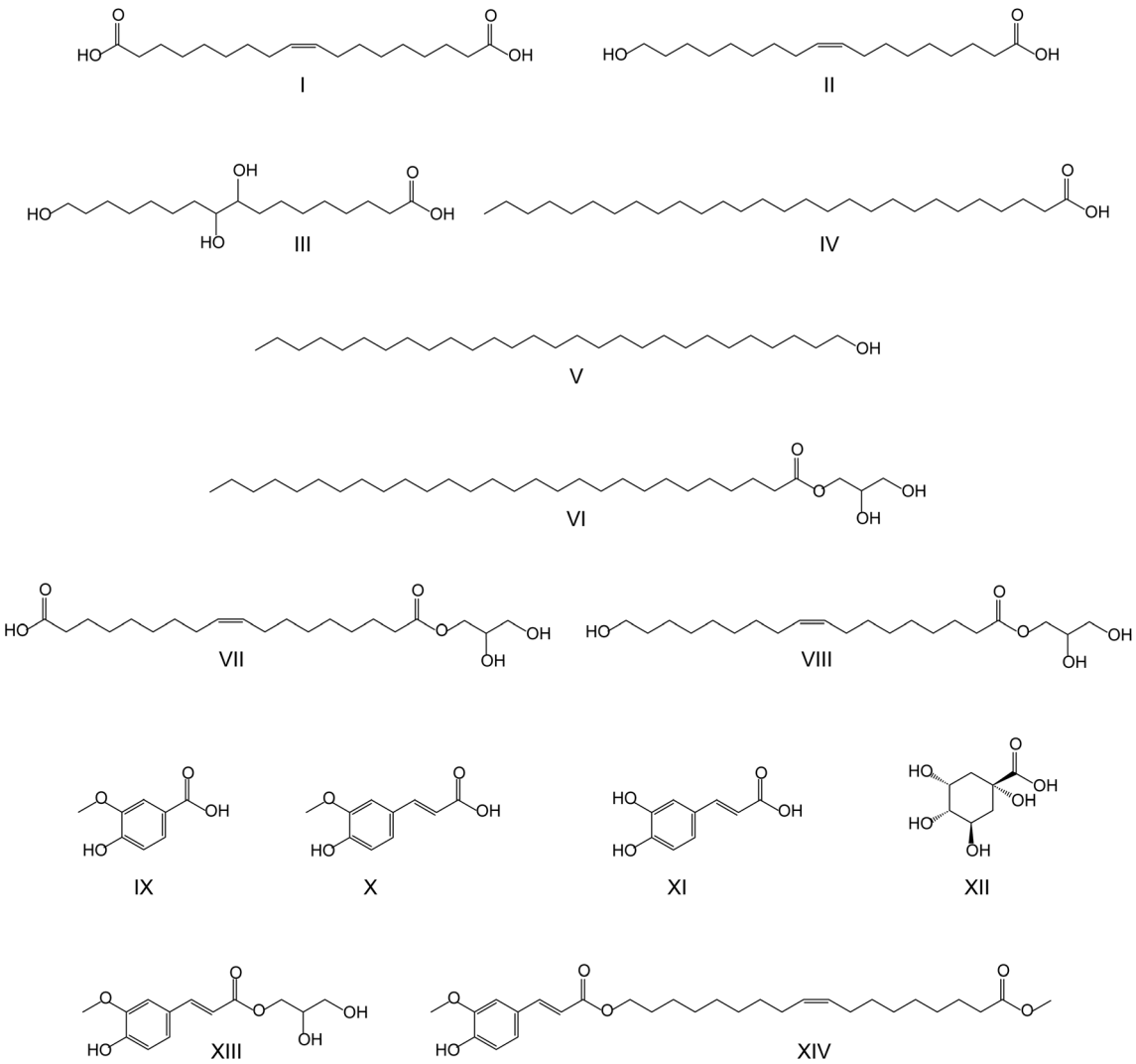

Fig. 4 Structures representative of the main compound classes identified and referred to in the text. **I**: octadec-9-ene-1,18-dioic acid; **II**: 18-hydroxyoctadec-9-enoic acid; **III**: 9,10,18-trihydroxyoctadecanoic acid; **IV**: *n*-octacosanoic acid; **V**: *n*-octacosanol; **VI**: 1-monooctacosanoylglycerol; **VII**: 1-mono(octadec-9-ene-18-oic acid-oyl)glycerol; **VIII**: 1-mono(18-hydroxyoctadec-9-enoyl)glycerol; **IX**: vanillic acid; **X**: ferulic acid; **XI**: caffeic acid; **XII**: quinic acid; **XIII**: glycerol ferulate; and **XIV**: 18-*O*-feruloyloxyoctadec-9-enoic acid methyl ester.

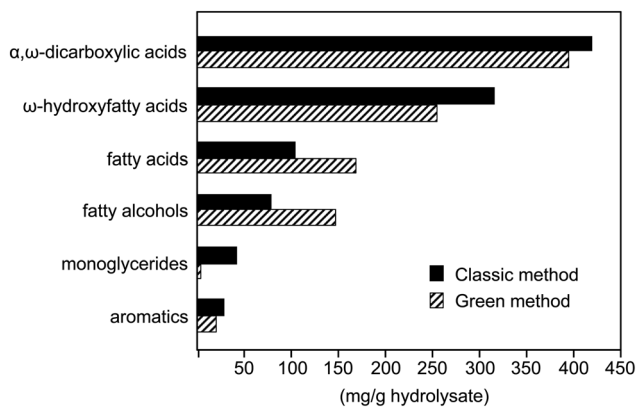

Fig. 5 Abundance (mg g^{-1} of hydrolysate) of the main families of compounds released from potato suberin using the classic and green methods.

Additionally, several di-and tri-hydroxyfatty acids were identified, including 9,10,18-trihydroxyoctadecanoic acid (**III**).

The series of fatty acids were found in the range from *n*-tetradecanoic acid (C_{14}) to *n*-dotriacontanoic acid (C_{32}), with a strong predominance of the even carbon-numbered homologues, and *n*-octacosanoic acid (C_{28}, **IV**) being the most predominant compound. Additionally, the unsaturated octadec-9-enoic (oleic, $C_{18:1}$) and octadeca-9,12-dienoic (linoleic, $C_{18:2}$) acids were also released, albeit in lower amounts.

Significant amounts of fatty alcohols were also found in the hydrolysates, particularly from the green method. The series extended from *n*-hexadecanol (C_{16}) to *n*-triacontanol (C_{30}), with strong predominance of the even carbon atom numbered homologues and *n*-octacosanol (C_{28}, **V**) being the most predominant alcohol released using both methods; no unsaturated alcohols were released.

Monoglycerides were released from both methods, with a higher yield using the classic method compared to the green one, where they were present in minor quantities, as discussed above. The classic method released different classes of monoglycerides, including monoacylglycerides of fatty acids, monoacylglycerides of ω-hydroxyfatty acids and monoacylglycerides of α,ω-dicarboxylic acids. In contrast, the green method exclusively released monoacylglycerides of fatty acids, specifically 1-monohexadecanoylglycerol (1-monopalmitin) and 1-monooctadecanoylglycerol (1-monostearin). In the classic method, monoacylglycerides of fatty acids ranged from 1-monohexadecanoylglycerol (C_{16}) to 1-monotriacontanoylglycerol (C_{30}), featuring only even carbon atom numbered homologues with the maximum for 1-monooctacosanoylglycerol (C_{28}, **VI**) and the absence of unsaturated fatty acids. The monoacylglycerides of α,ω-dicarboxylic acids released were primarily represented by 1-mono(octadec-9-ene-18-oic acid-oyl)glycerol (**VII**) (both in its free form and as its methyl ester), with minor amounts of the 2-mono(octadec-9-ene-18-oic acid-oyl)glycerol isomers. Similarly, monoacylglycerides of ω-hydroxyfatty acids predominantly comprised 1-mono(18-hydroxyoctadec-9-enoyl)glycerol (**VIII**) alongside minor amounts of its 2-mono(18-hydroxyoctadec-9-enoyl)glycerol isomer.

Finally, various aromatic compounds were identified, including vanillic acid (**IX**), ferulic acid (**X**), and caffeic acid (**XI**), alongside quinic acid (**XII**), which is produced from the hydrolysis of chlorogenic acid. Furthermore, several feruloyl esters were also identified. For example, glycerol ferulate (**XIII**) was released exclusively using the classic method. In contrast, a series of *n*-alkylferulates, ranging from *n*-hexadecylferulate (C_{16}) to *n*-tetracosanylferulate (C_{24}), was released solely through the green method, albeit in very small amounts, likely due to their partial hydrolysis. These alkylferulates are extractives present in significant amounts in the potato peel and were largely removed during the solvent extraction steps of the classical method. Moreover, significant amounts of feruloyl esters of ω-hydroxyfatty acids, particularly 18-*O*-feruloyloxyoctadec-9-enoic acid methyl ester (**XIV**), were released using the classic method but were absent when using the green method.

Determination of α-solanine and α-chaconine in the hydrolysates

The steroidal glycoalkaloids α-solanine and α-chaconine, Fig. 6, are naturally occurring toxins found in potato peels that pose potential health risks to humans. As the hydrolysates derived from potato peels are being considered for polymer production for food packaging applications, there is concern that these toxic compounds may become concentrated in the hydrolysates during processing. Therefore, it is important to evaluate the presence of these glycoalkaloids in the hydrolysates obtained from suberin-rich potato peel waste. To address this concern, the levels of α-solanine and α-chaconine were

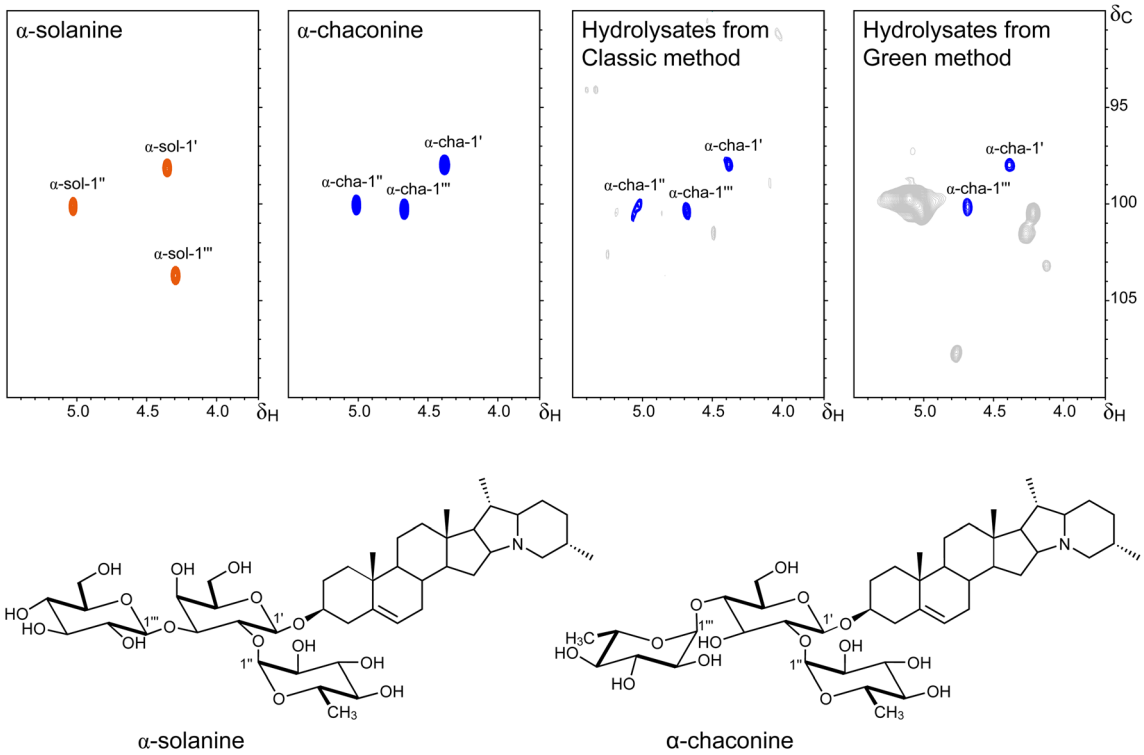

Fig. 6 Quantification of the glycoalkaloids α-solanine and α-chaconine in the hydrolysates obtained *via* the classic and green methods using 2D NMR spectroscopy. Anomeric regions (δ_C/δ_H 90–110/3.7–5.5 ppm) of the 2D HSQC NMR spectra in DMSO-d_6 highlighting the signals for the anomeric carbons of pure α-solanine and α-chaconine, along with those detected in the hydrolysates obtained using both methods. The chemical structures of α-solanine and α-chaconine are shown below.

estimated using 2D-NMR spectroscopy. Characteristic signals were observed in the anomeric region of the spectra, Fig. 6, corresponding to the anomeric carbons of the glycoalkaloids. These signals served as distinctive markers for quantitative analysis, which was carried out by integrating the corresponding signals from samples with known concentrations of glycoalkaloids. The NMR results revealed that only α-chaconine was detected in the hydrolysates obtained using both the classic and green methods, though in trace amounts (less than 0.1% in both cases); no traces of α-solanine were detected in any of the hydrolysates. In this case, most of the glycoalkaloids might have been largely removed during the extraction steps preceding the hydrolysis. In the classic method, these toxins could be largely eliminated during the ethanol, water, and methanol extractions. In the green method, which employs only a water pre-extraction, most glycoalkaloids could be similarly removed, due to their amphiphilic character and polar sugar moieties, with the remainder likely eliminated during the alkaline hydrolysis step. This last observation is consistent with the known behavior of steroidal glycoalkaloids, which tend to precipitate under basic conditions such as those used during hydrolysis.[21]

Polymer coatings from "green" suberin-rich hydrolysate: a proof-of-concept

Fig. 7A shows a representative photograph of the coatings obtained from the suberin-rich hydrolysate before and after thermal polymerization at 175 °C for 60 minutes. The unpolymerized coating exhibits a lighter, matte appearance, whereas the polymerized sample displays a darker yellow-brown coloration and a more homogeneous surface. In fact, the colorimetric parameters (CIELAB) revealed a noticeable darkening and chromatic shift upon thermal polymerization of the suberin-based coating. The luminosity (L^*) decreased from 76.0 to 71.2, whereas both a^* and b^* increased from 1.2 to 5.9 and from 24.2 to 31.5, respectively, indicating a transition toward a warmer reddish-yellow hue. These variations were quantitatively supported by a sharp increase in the Browning Index (BI) from 1.7 to 34.3 and a total color difference (ΔE) of 9.9*, corresponding to a visually perceptible change. The observed chromatic evolution is consistent with the formation of conjugated and partially oxidized structures during thermal curing at 175 °C.[25] The darker, yellow-reddish appearance of the polymerized coating thus reflects the chemical transformations underlying its polymer network formation.

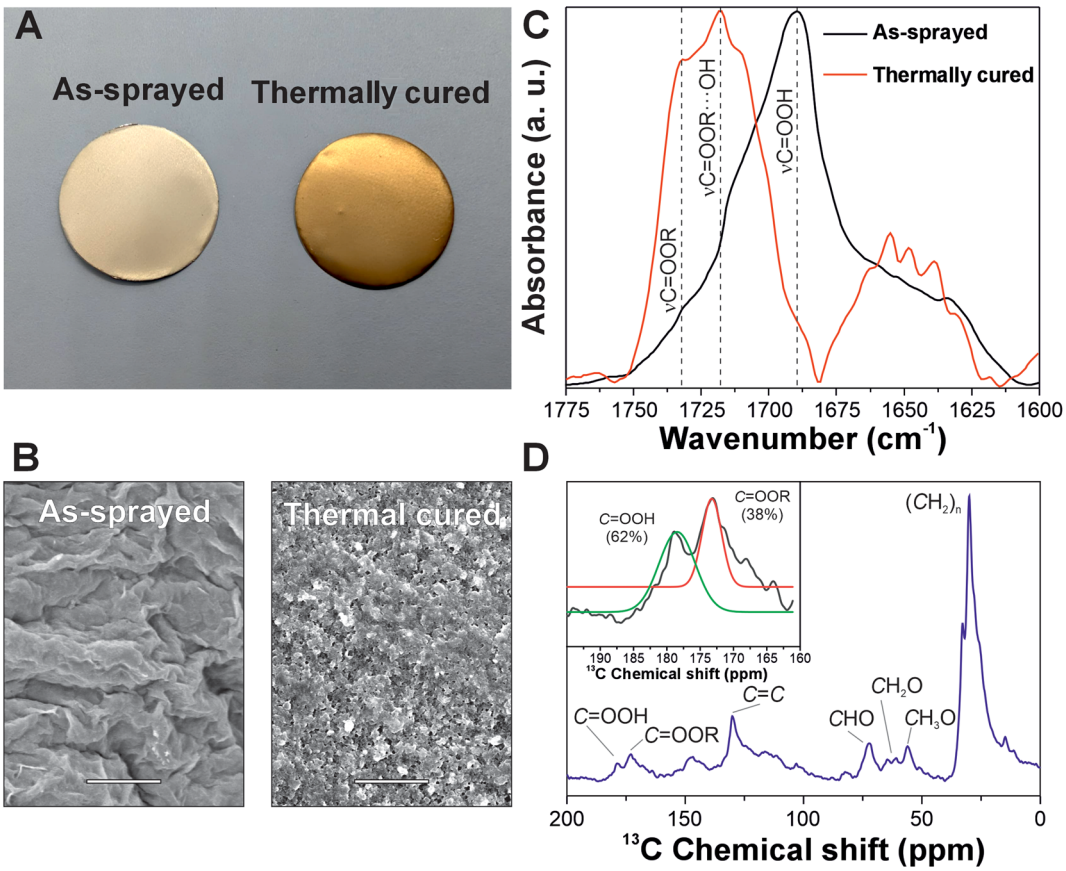

Fig. 7 (A) Photographic images of the as-sprayed and the thermally cured (*i.e.*, polymerized) coatings. (B) Top-view SEM images of the as-sprayed and thermally cured coatings. Scale bar: 20 μm. (C) ATR-FTIR spectra of the as-sprayed and thermally cured coatings in the 1775–1600 cm^{-1} spectral region. Main assignments are included. (D) ^{13}C NMR spectrum of the thermally cured coating. Main assignments are included. The inset shows the deconvolution of the signal ascribed to carboxyl and ester groups.

The surface morphology of the coatings was investigated by SEM, Fig. 7B. The unpolymerized coating, Fig. 7B left, exhibited a heterogeneous and wrinkled surface characterized by overlapping lamellar features and pronounced roughness at the micrometric scale. Although the layer appears largely continuous, the presence of irregular domains and occasional agglomerated fragments indicates limited coalescence and cohesion, consistent with a physically deposited film. In contrast, the thermally polymerized coating, Fig. 7B right, presents a more compact and particulate morphology, with coalesced granular domains. This microstructural evolution reflects material rearrangement and densification during thermal curing.

The thermal polymerization performed at 175 °C for 60 min in the melt state was monitored by ATR-FTIR spectroscopy. Fig. 7C shows the carbonyl stretching region (1775–1600 cm^{-1}) of the coatings before and after curing. The spectrum of the as-sprayed coating was dominated by an intense band centered at approximately 1690 cm^{-1}, assigned to the C═O stretching vibration of hydrogen-bonded carboxylic acid groups.[26] After thermal curing, this band underwent a marked shift toward higher wavenumbers, giving rise to two main contributions at approximately 1719 and 1731 cm^{-1}, attributed to the C═O stretching modes of hydrogen-bonded ester groups and free ester carbonyls, respectively.[27] This evolution reflects the conversion of carboxylic acids into ester linkages and the concomitant reduction of acid–acid hydrogen bonding, providing spectroscopic evidence of melt-polycondensation between suberin-derived monomers.

To further characterize the thermally polymerized coating, solid-state ^{13}C NMR spectroscopy was employed, Fig. 7D. The main resonances were assigned as follows: long-chain aliphatic methylenes $(CH_2)_n$ at ~30 ppm, methoxy carbons (CH_3O) at ~56 ppm, alkoxy methylenes (CH_2O) at ~64 ppm, secondary alcohol carbons (CHO) at ~72 ppm, olefinic carbons (C═C) at ~130 ppm, ester carbonyls (C═OOR) at ~173 ppm, and carboxylic acid carbonyls (C═OOH) at ~179 ppm.[28] These signals are consistent with the chemical fingerprint of partially esterified suberin-derived monomers forming a polyester network. To estimate the extent of esterification, the carbonyl region was deconvolved into contributions from ester (C═OOR) and carboxylic acid (C═OOH) groups (inset of Fig. 7D). The analysis revealed that approximately 38% of the carbonyl functionalities correspond to ester groups, indicating partial conversion during the melt-polycondensation. This outcome can be attributed to an excess of carboxylic acid groups relative to hydroxyl groups in the hydrolyzate, in agreement with the compositional data reported in Table 1.

Conclusions

In this study, suberin-rich potato peel waste, a widely available agro-industrial by-product, was successfully valorized as a renewable feedstock for the extraction of multifunctional aliphatic and aromatic compounds. Two hydrolytic strategies were investigated: a well-established classic method based on methanolysis using sodium methoxide and a novel green approach based on aqueous NaOH hydrolysis. The green method was optimized by response surface methodology evaluating the effects of temperature, reaction time, and base concentration, with optimal conditions identified as 0.5 M NaOH, 85 °C, and 2 h, achieving recovery yields of ~20% of the initial biomass.

Compositional analysis of the hydrolysates by GC-MS revealed that the green extraction method produced a complex mixture of α,ω-dicarboxylic acids, ω-hydroxyfatty acids, fatty alcohols, free fatty acids, and aromatic derivatives. The green method presented several key advantages: (i) slightly higher overall monomeric yields compared to those with the classic sodium methoxide-based methanolysis, (ii) elimination of organic solvents and flammable reagents, (iii) preservation of a broader array of low-polarity compounds, (iv) preservation of free carboxylic groups, thus improving their suitability as potential building blocks for polymer production, and (v) significant reduction of glycoalkaloid (α-solanine and α-chaconine) content, enhancing the safety of the resulting materials.

The direct melt polycondensation of the green suberin-rich hydrolysate into polymer coatings emphasizes the practical potential of the recovered multifunctional monomers for sustainable material fabrication, establishing a complete valorization route from agro-industrial waste to bio-based coatings.

These results highlight the potential of aqueous alkaline hydrolysis as a greener, safer, and scalable alternative for suberin depolymerization in complex agro-waste, paving the way for the development of sustainable materials and chemicals from potato processing residues.

Author contributions

Pedro Florido-Moreno: methodology and data curation. Diego Rodríguez-Rodríguez: methodology and resources. José J. Benítez: methodology, funding acquisition, and resources. Jorge Rencoret: methodology and resources. Ekram Wassel: methodology and resources. Ruth E. Stark: methodology and resources. Susana Guzman-Puyol: methodology and resources. José A. Heredia-Guerrero: conceptualization, data curation, funding acquisition, methodology, project administration, resources, and writing – original draft. José C. del Río: conceptualization, data curation, methodology, resources, and writing – original draft.

Conflicts of interest

There are no conflicts to declare.

Data availability

The data supporting this article have been included as part of the supplementary information (SI). Supplementary information is available. See DOI: https://doi.org/10.1039/d6gc00954a.

Acknowledgements

This work was supported by the Spanish Ministerio de Ciencia, Innovación y Universidades/Agencia Estatal de Investigación (MICIU/AEI/10.13039/501100011033) through the projects RYC2023-042483-I and PID2023-152543OB-I00, cofinanced by the European Regional Development Fund (ERDF) "A way to make Europe". Additional support was provided by the project TED2021-129656B-I00, funded by the Spanish MICIU/AEI/10.13039/501100011033, the European Union's "NextGenerationEU"/PRTR initiative, and a PROLAB early career fellowship award from the American Society of Biochemistry and Molecular Biology. NMR instrumentation at he New York Structural Biology Center was obtained through a grant from U.S. National Institutes of Health (NIH) Equipment Grant (S10OD030373).

The authors thank El Tío de las Papas S.L. for kindly providing the potato peels used in this study.

References

1 C. G. Otoni, H. M. C. Azeredo, B. D. Mattos, M. Beaumont, D. S. Correa and O. J. Rojas, *Adv. Mater.*, 2021, **33**, 2102520.
2 L. Yang, X.-C. Wang, M. Dai, B. Chen, Y. Qiao, H. Deng, D. Zhang, Y. Zhang, C. M. Villas Bôas de Almeida, A. S. F. Chiu, J. J. Klemeš and Y. Wang, *Energy*, 2021, **228**, 120533.
3 A. J. Ragauskas, C. K. Williams, B. H. Davison, G. Britovsek, J. Cairney, C. A. Eckert, W. J. Frederick, J. P. Hallett, D. J. Leak, C. L. Liotta, J. R. Mielenz, R. Murphy, R. Templer and T. Tschaplinski, *Science*, 2006, **311**, 484–489.
4 L. de S. C. Carnaval, A. K. Jaiswal and S. Jaiswal, *J. Compos. Sci.*, 2024, **8**, 41.
5 C. Fritsch, A. Staebler, A. Happel, M. A. C. Márquez, I. Aguiló-Aguayo, M. Abadias, M. Gallur, I. M. Cigognini, A. Montanari, M. J. López, F. Suárez-Estrella, N. Brunton, E. Luengo, L. Sisti, M. Ferri and G. Belotti, *Sustainability*, 2017, **9**, 1492.
6 A. Vinod, M. R. Sanjay, S. Suchart and P. Jyotishkumar, *J. Cleaner Prod.*, 2020, **258**, 120978.
7 L. Singh, S. Kaur, P. Aggarwal and N. Kaur, *Int. J. Food Sci. Technol.*, 2023, **58**, 2686–2694.
8 S. J. Vishwanath, C. Delude, F. Domergue and O. Rowland, *Plant Cell Rep.*, 2015, **34**, 573–586.
9 J. Graça, *Front. Chem.*, 2015, **3**, 62.
10 A. Gandini, C. Pascoal Neto and A. J. D. Silvestre, *Prog. Polym. Sci.*, 2006, **31**, 878–892.
11 M. A. Bernards, *Can. J. Bot.*, 2002, **80**, 227–240.
12 J. Graça and H. Pereira, *J. Agric. Food Chem.*, 2000, **48**, 5476–5483.
13 P. E. Kolattukudy, in *Biopolymers Online*, 2005.
14 R. Ferreira, H. Garcia, A. F. Sousa, C. S. R. Freire, A. J. D. Silvestre, L. P. N. Rebelo and C. Silva Pereira, *Ind. Crops Prod.*, 2013, **44**, 520–527.
15 R. Ferreira, H. Garcia, A. F. Sousa, M. Guerreiro, F. J. S. Duarte, C. S. R. Freire, M. J. Calhorda, A. J. D. Silvestre, W. Kunz, L. P. N. Rebelo and C. Silva Pereira, *RSC Adv.*, 2014, **4**, 2993–3002.
16 A. Karnaouri, U. Rova and P. Christakopoulos, *Molecules*, 2016, **21**, 427.
17 D. Schrenk, M. Bignami, L. Bodin, J. K. Chipman, J. del Mazo, C. Hogstrand, L. R. Hoogenboom, J.-C. Leblanc, C. S. Nebbia, E. Nielsen, E. Ntzani, A. Petersen, S. Sand, T. Schwerdtle, C. Vleminckx, H. Wallace, L. Brimer, B. Cottrill, B. Dusemund, P. Mulder, G. Vollmer, M. Binaglia, L. Ramos Bordajandi, F. Riolo, R. Roldán-Torres and B. Grasl-Kraupp, *EFSA J.*, 2020, **18**, e06222.
18 A. F. Sánchez Maldonado, E. Mudge, M. G. Gänzle and A. Schieber, *Food Res. Int.*, 2014, **65**, 27–34.
19 I. Martínez-García, C. Gaona-Scheytt, S. Morante-Zarcero and I. Sierra, *Foods*, 2024, **13**, 651.
20 V. Romanucci, G. Di Fabio, C. Di Marino, S. Davinelli, G. Scapagnini and A. Zarrelli, *Phytochem. Lett.*, 2018, **23**, 116–119.
21 L. E. Rodriguez-Saona, R. E. Wrolstad and C. Pereira, *J. Food Sci.*, 1999, **64**, 445–450.
22 R. Järvinen, A. J. D. Silvestre, U. Holopainen, M. Kaimainen, A. Nyyssölä, A. M. Gil, C. Pascoal Neto, P. Lehtinen, J. Buchert and H. Kallio, *J. Agric. Food Chem.*, 2009, **57**, 9016–9027.
23 J. Rencoret, S. Guzmán-Puyol, J. J. Benítez, J. A. Heredia-Guerrero and J. C. del Río, *Ind. Crops Prod.*, 2025, **236**, 122116.
24 R. Järvinen, H. Rauhala, U. Holopainen and H. Kallio, *LWT-Food Sci. Technol.*, 2011, **44**, 1355–1361.
25 J. J. Benítez, S. Guzman-Puyol, M. A. Cruz-Carrillo, L. Ceseracciu, A. González Moreno, A. Heredia and J. A. Heredia-Guerrero, *Front. Chem.*, 2019, **7**, 643.
26 L. Bellamy, *The infra-red spectra of complex molecules*, Springer Science & Business Media, 2013.
27 J. J. Benítez, M. C. Ramírez-Pozo, M. M. Durán-Barrantes, A. Heredia, G. Tedeschi, L. Ceseracciu, S. Guzman-Puyol, D. Marrero-López, A. Becci, A. Amato and J. A. Heredia-Guerrero, *J. Cleaner Prod.*, 2023, **386**, 135836.
28 O. Serra, S. Chatterjee, M. Figueras, M. Molinas and R. E. Stark, *Biomacromolecules*, 2014, **15**, 799–811.